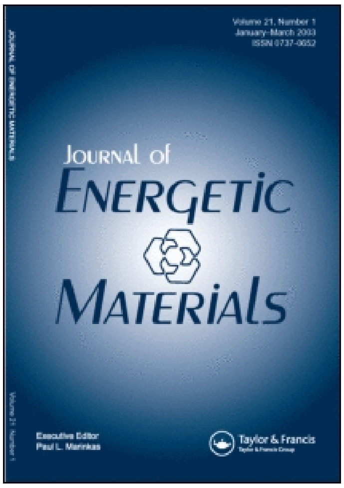

Journal of Energetic Materials
Publication details, including instructions for authors and subscription information:
http://www.informaworld.com/smpp/title~content=t713770432

Dynamic Measurement of the Permeability of an Explosive Undergoing Thermal Damage

B. W. Asay; G. Parker; P. Dickson; B. Henson; L. Smilowitz

To cite this Article Asay, B. W. , Parker, G. , Dickson, P. , Henson, B. and Smilowitz, L.(2004) 'Dynamic Measurement of the Permeability of an Explosive Undergoing Thermal Damage', Journal of Energetic Materials, 22: 1, 25 — 39
To link to this Article: DOI: 10.1080/07370650490438284
URL: http://dx.doi.org/10.1080/07370650490438284

Energetic Materials, 21: 25–39, 2004

ISSN: 0737-0652 print
DOI: 10.1080/07370650490438284

Dynamic Measurement of the Permeability of an Explosive Undergoing Thermal Damage

B. W. ASAY
G. PARKER
P. DICKSON
B. HENSON
L. SMILOWITZ

Los Alamos National Laboratory,
Los Alamos, NM, USA

We have constructed a gas permeameter to measure the permeability of explosives that have been thermally damaged. We report on the calibration of the instrument, as well as measurements of the permeability of PBX 9501, a plastic bonded explosive. The limitations of this technique are shown, as well as the effects that crystalline phase transition, volumetric expansion, and chemical reaction have on the permeability of this material.

Keywords: PBX, permeability

Introduction

Thermal damage can have a profound effect on the physical as well as the chemical state of an explosive. In addition to thermal expansion, there can be phase change effects (e.g., beta to delta transition in HMX) that can cause micro- and macro-cracking along with porosity generation. The additional surface area,

Address correspondence to Blaine W. Asay, MS C920, Los Alamos National Laboratory, Los Alamos, NM 87545. E-mail: bwa@lanl.gov

which results from the physical damage, contributes greatly to the behavior if ignition and subsequent combustion of the material occurs [1]. To predict the material response successfully, reliable and accurate models of the material's equation of state are required, in addition to thermal transport properties, chemical kinetics, and many other details. In explosives where gas phase reactions play a major role in the energy release, it is particularly important to understand diffusive and convective gas transport. However, reliable measurements of the permeability (K) of damaged explosives are not currently available, and thus rough estimates have been used in calculations. Because the rate at which gas diffuses through a system is directly proportional to the permeability, errors in this quantity have a very large effect on the final predictions of system response.

It is highly desirable to determine the relationship between permeability and porosity. Many different relationships have been proposed, but, in fact, a generalized relation is not possible because, as demonstrated by the work of Rumpf and Gupte, K depends on the particle size distribution [2]. Also, K, as well as the porosity function, depend on the particle shape and the packing structure. Because these parameters vary widely between systems and, in fact, may also vary within heterogeneous systems, the most that can be hoped for is an accurate measurement of K in the material of choice under well-controlled conditions.

We have constructed an instrument that measures the permeability of explosives in both static and dynamic environments. We report here the calibration of the system using rock core specimens and measurements in explosive samples that have been thermally damaged using two different techniques.

Theory

Permeability is defined by Darcy's law, which is an empirical function that arose through observation of the behavior in porous systems. It has been shown to be widely applicable in regions of laminar flow but breaks down at higher velocities and in rarified (extremely low–pressure) systems. The Reynolds number (Re) has been used to determine whether or not conditions are appropriate. However, the definition of Re in porous systems varies. Collins [3] defines it as

$$\mathrm{Re} = \frac{Q\rho\delta}{\mu A \varepsilon}, \tag{1}$$

where Q is the volumetric flow rate, ρ is the density, μ is viscosity, δ is the average particle diameter, A is the cross-sectional area, and ε is the porosity. Unfortunately in many systems the particle dimensions are not known. Also, even if it is known, the average particle diameter may not represent a useful quantity. The American Petroleum Institute (API) recommends the following definition of Re:

$$\mathrm{Re} = \frac{dQ\rho}{\mu A}, \tag{2}$$

where d is the conduit diameter. This definition avoids ambiguities of particle dimensions. Scheidegger [4] points out that the notion of hydraulic radius theory (upon which Re and friction factor concepts are based) is dependent on determining an effective diameter, and that is impossible to do. With these uncertainties there is no agreed upon Re indicating a transition region above which Darcy's law is invalid. There are tests of the data using a variety of methods that show whether or not Darcy flow is obtained, but in general each case must be treated separately. This is not an unimportant point, as the API concludes that failure to maintain purely viscous flow is the single-most common source of error in the measurement of permeability. It seems clear from the evidence, however, that the law is valid only for very low percolation velocities. The ASTM Procedure [5] states that exit flow rates less than 1 cm/s are usually satisfactory, and all data reported here meet that criterion.

We will describe first the general theory and then show our adaptation to accommodate our specific implementation. Permeability is a general term used to describe the conductivity of a fluid in a porous system. However, it varies with fluid and the mechanism of permeation. To separate out the effects of the fluid, *specific* permeability (k) is defined as

$$k = K\mu. \tag{3}$$

For an inclined system using an incompressible liquid in slow unidirectional flow, the integral form of Darcy's law, following Dullien [2], can be written as

$$Q = -\frac{kA}{\mu}\frac{[\Delta(P+\rho gh)]}{L}, \tag{4}$$

where P is the pressure, g is the acceleration due to gravity, h is the vertical distance, and L is the length. For gases, a differential form is used to account for compressibility. While there is no unique way of arriving at this form, an accepted relationship is

$$v = -\frac{k}{\mu}(\nabla P - \rho g), \tag{5}$$

where v is Q/A. In our application $\rho g << \nabla P$ and can be neglected.

Thus, with constant pressures and temperature at the entrance and exit, permeability can be directly calculated from a measurement of the flow rate. However, this measurement can constitute a major source of error, as it is difficult to do reliably. Shepherd and Begeal [6] measured flow rates indirectly assuming a quasi-steady pressure. We have followed a similar treatment.

From Equation (5) we have

$$v = -\frac{k}{\mu}\frac{\mathrm{d}P}{\mathrm{d}x}. \tag{6}$$

Using the fact that at a given location the mass flow rate is constant, and using the ideal gas law, we obtain

$$\frac{RT}{PA}n' = v = -\frac{k}{\mu}\frac{\mathrm{d}P}{\mathrm{d}x}, \tag{7}$$

where n' is the mass flow rate. Integrating both sides,

$$\frac{RT}{PA} n' \int_{x_1}^{x_2} dx = -\frac{k}{\mu} \int_{P_1}^{P_2} dP, \tag{8}$$

and then replacing the mass flow with velocity, we obtain for two specific locations

$$v_2 = -\frac{k}{\mu} \frac{P_2^2 - P_1^2}{2P_2 L} \quad \text{or} \quad v_1 = -\frac{k}{\mu} \frac{P_2^2 - P_1^2}{2P_1 L} \tag{9}$$

where the subscripts 2 and 1 represent the exit and entrance, respectively.

Equation (9) is the standard equation used in defining permeability in systems using gas as the working fluid. Sutherland's equation [7] was used to account for viscosity dependence on temperature:

$$\mu_1 = \frac{K T_1^{3/2}}{T_1 + C} \quad \text{or} \quad \mu_2 = \frac{K T_2^{3/2}}{T_2 + C}, \tag{10}$$

where the subscripts 2 and 1 represent different temperature states, T is temperature in Kelvin, and C and K are constants for nitrogen gas equaling 102.0 and 1.385×10^{-5} respectively.

In a typical device one sets the reservoir and outlet pressure at constant values and then measures the gas flow rate using an orifice plate or other method. An alternative technique is to use a variable reservoir pressure and then calculate the flow rate, assuming that the pressure is quasi-steady. In this case we calculate the mass flow and velocity at the exit as

$$\frac{dn}{dt} = \frac{dP_r}{dt} \frac{V_r}{RT_r}, \tag{11}$$

$$v_2 = \frac{dn}{dt} \frac{RT}{PA} \tag{12}$$

where the subscript r refers to the reservoir state. This velocity is then used in Equation (9) to calculate the permeability of the sample at the exit.

Experimental

A permeameter was constructed that permits quantitative dynamic measurement of gas flow through a specimen. The permeameter consists of a supply reservoir, calibration reservoir, specimen holder, pressure transducers, and thermocouples (see schematic in Figure 1). Test specimens are machined or pressed into cylinders with a diameter of 1 cm and lengths varying between 2.6 and 3 cm. The samples are potted in a 0.75 inch Swagelock® port connector using JB Weld®epoxy. A thermocouple is embedded in the epoxy next to both ends of the specimen before curing. Once cured, the specimen holder is attached to the permeameter, wrapped in electric heating tape, and then overwrapped with fiberglass insulation. Because viscosity and permeability are each temperature dependent, a uniform temperature profile throughout the sample was required. This was accomplished by heating using a temperature controller and monitoring with the two thermocouples at either end. The mass flow rates of the gas through the sample were very low

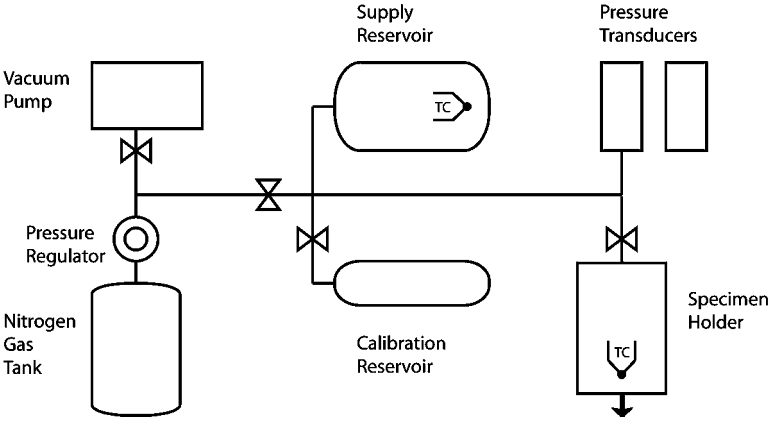

Figure 1. Schematic of dynamic permeameter.

(~0.6–6 µmoles/s), thus ensuring gas temperature equilibration with the heated sample matrix. All results were obtained from experiments with less than 3°C difference between sample inlet and outlet.

The volume of the calibration reservoir is determined by measuring the mass of isopropyl alcohol required to fill the reservoir completely. The system volume is then calculated from differential pressure measurements. The system volume is known to ± 0.5%. During an experiment simultaneous temperature and pressure measurements of the reservoir, sample, and ambient atmosphere are logged at 1 s scan intervals. Temperature is logged with an Omega® Tempscan 1100. Absolute pressure of the system and the atmosphere are measured with a pair of electronic pressure transducers (Omega® PX01C1-100AI and PX01C1-500AI). Voltage is recorded with an Omega® Tempscan 1100 equipped with a voltage board. Accuracy of the voltages is ± 0.2%.

Proper functioning of the permeameter was verified using five rock core specimens of known permeabilities. These specimens were also sent to an independent laboratory for analysis; the results are shown in Table 1. These data provide an indication of the amount of scatter that can be expected in making measurements of this nature. Agreement within one order of magnitude can be expected, especially at low values of permeability.

Table 1
Verification against rock core specimens

Sample ID	Rocktell k (m^2)	ATT k (m^2)	LANL k (m^2)
LA001	6.12×10^{-15}	N/A	1.65×10^{-15}
LA002	1.01×10^{-14}	N/A	3.85×10^{-15}
LA003	9.53×10^{-16}	2.85×10^{-16}	1.88×10^{-16}
LA004	1.94×10^{-15}	5.75×10^{-16}	5.15×10^{-16}
LA005	1.73×10^{-16}	2.65×10^{-17}	3.42×10^{-17}

Values from Rocktell were offset consistently higher than ours, which agreed well with ATT. Rocktell's discrepancies are unexplained.

After leak testing and calibration, experiments were conducted with nitrogen gas (99.995% purity) using pristine and thermally damaged PBX 9501 explosive (95% by weight HMX, 2.5% estane binder, and 2.5% nitroplasticizer), as well as a simulant having similar properties, which was developed to assess the effects of HMX phase transition on permeability. This simulant was composed of 95% by weight ammonium sulfate (density of 1.77 g/cc, pressed to 96% of the theoretical maximum density, bimodal particle size distribution, and chemically inert at experimental temperatures), 2.5% estane binder, and 2.5% nitroplasticizer.

Temperature and pressure data as a function of time were acquired, numerical derivatives were obtained, and the specific permeability was calculated as described above.

Results and Discussion

Sensitivity and Error

Error in these experiments arises from electronic noise, uncertainty in system volume, and instrument error. A permeability of $10^{-19}\,\mathrm{m}^2$ results in a depressurization rate of only 0.0250 kPa/hr. A measure of the upper limit of sensitivity was derived by measuring $\mathrm{d}p/\mathrm{d}t$ using an impermeable steel plug as the sample and then calculating an effective permeability. This resulted in data exhibiting stochastic oscillations to either side of $\phi\,\mathrm{m}^2$ (theoretically impermeable). Variation resulting in negative permeability values is not real and is therefore treated as an indicator of a sum of the electronic and instrument error. The magnitude of error was averaged from three repetitions and found to be 1.77×10^{-19} ($\sigma = 3.39 \times 10^{-19}\,\mathrm{m}^2$). This result indicates that the instrument is incapable of measuring values lower than that value. A summary of the data taken in this study, which will be described below, is found in Table 2.

Pristine PBX 9501

Experiments were performed testing undamaged, machined PBX 9501 at room temperature to establish a baseline

Table 2
Summary of data

		Average permeability (m^2), error $\pm 1.77 \times 10^{-19}$ m^2		
	Sample ID	20°C	150°C	180°C
PBX 9501	Potted before damage	4.16×10^{-19}	N/A	2.89×10^{-16}
	Potted after damage	6.88×10^{-14}	3.04×10^{-15}	1.17×10^{-15}
Simulant	Potted before damage	3.36×10^{-18}	N/A	2.45×10^{-16}
	Potted after damage	1.48×10^{-15}	5.70×10^{-16}	2.46×10^{-15}
Steel plug		1.77×10^{-19}	N/A	N/A

permeability value for the explosive. These data were averaged and found to be very near the sensitivity limit of the permeameter at 4.16×10^{-19} ($\sigma = 1.91 \times 10^{-19}\,\mathrm{m}^2$).

PBX 9501 Damaged with Confinement

Confinement is a significant variable in these experiments because both thermal expansion and the volume increase of the HMX crystals resulting from the $\beta - \delta$ phase transition could potentially cause compression of the heated sample and affect the measured permeability. Samples were constructed in two ways. In the first, the sample was heated the desired amount of time, cooled, and then potted into the fixture. In the second, the sample was potted and then heated while mounted in the permeameter.

Samples potted in pristine condition were subsequently heated to 180°C and held at temperature for periods of 2–20 hr. Upon heating, pressure would begin to drop at an increasing rate for approximately 2–3 hr, after which there was an observed exponential pressure-decay regime (Figure 2). Data from this regime, where the pressure is assumed quasi-steady (Figure 3), were used to calculate permeability of radially confined PBX 9501 undergoing thermal damage. We found that permeability increases initially by three orders of magnitude to $2.89 \times 10^{-16}\,\mathrm{m}^2$ after 2–3 hr at 180°C. During the quasi-steady regime, permeability continues to rise, though not significantly. This may indicate a secondary mechanism of damage that is not yet understood. Finally, upon cooling and sample contraction, dramatic increases in permeability were observed; however, the current experimental design does not control for this condition, and these data will not be addressed at this time.

PBX 9501 Damaged Unconfined

To eliminate the effects of radial confinement on samples undergoing damage, several samples were damaged unconfined to allow for unhindered expansion. After cooling, they were

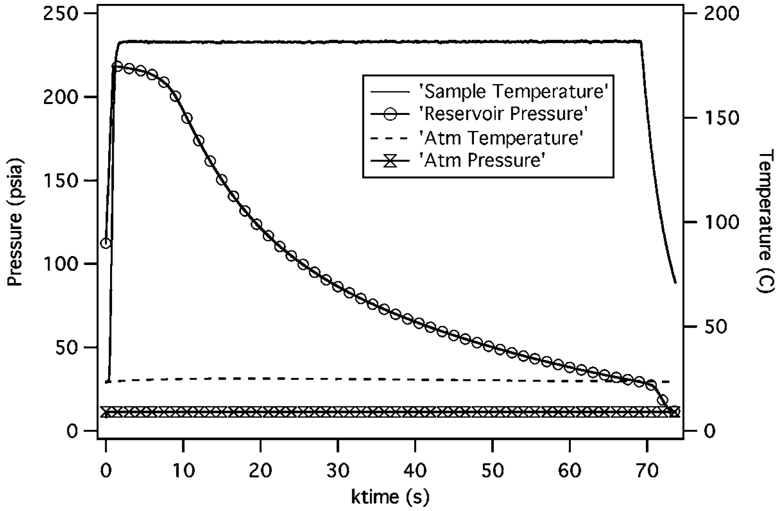

Figure 2. Raw data set used to calculate permeability. Data from a typical sample damaged with confinement.

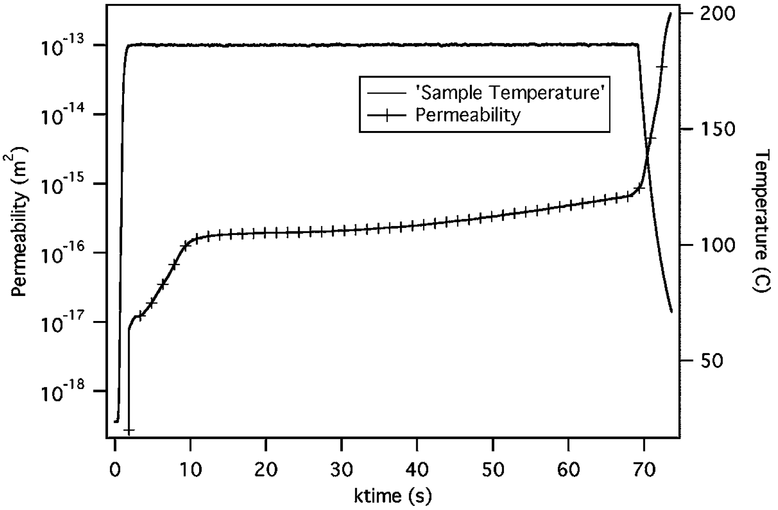

Figure 3. Data from Figure 2 converted to permeability. Temperature is also plotted for correlation.

potted, and permeability was measured at $6.88 \times 10^{-14}\,\mathrm{m}^2$, which is five orders of magnitude greater than pristine PBX 9501. Upon reheating these samples to 150 and 180°C, permeability decreased by ~1–1.5 orders of magnitude at $3.04 \times 10^{-15}\,\mathrm{m}^2$ and $1.17 \times 10^{-15}\,\mathrm{m}^2$, respectively (Figure 4). When compared to PBX 9501 damaged in confinement, one can see that the confined samples were 10 times less permeable at 180°C, indicating the compressive effects of thermal expansion and/or phase change in confined samples to be real and significant. The same result was obtained with the simulant that did not undergo phase transition (see next section).

Results Using Simulant

The preceding experiments were repeated with the simulant, with two notable differences in sample structure. First, the

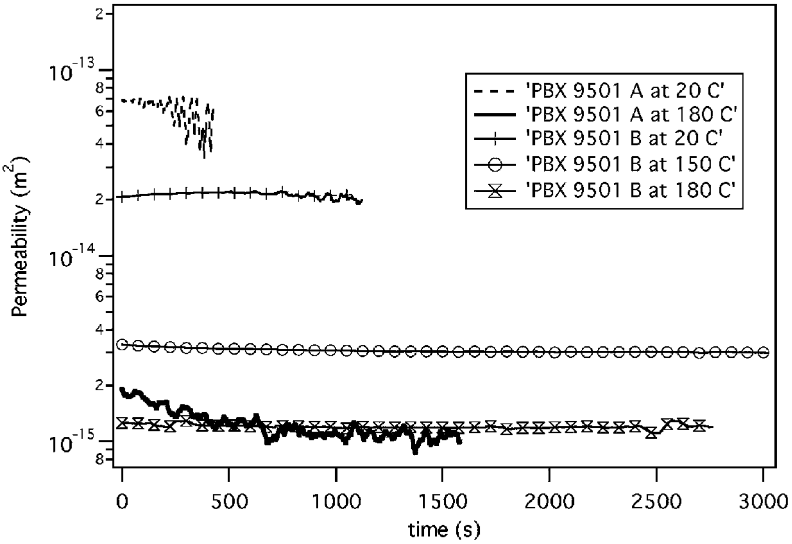

Figure 4. Comparison of permeability measured at 20, 150, and 180°C of two PBX 9501 samples that were damaged unconfined. A and B are separate identical samples.

simulant was die-pressed into cylinders, whereas the PBX 9501 was machined from isostatically pressed billets, possibly resulting in variation in HMX crystal size distributions and packing densities within individual samples. Second, the simulant was only 96% of its theoretical maximum density (TMD), whereas PBX 9501 is typically 98% TMD. Extending this point, the simulant initially has 4% porosity, whereas PBX 9501 has 2% porosity. As expected for samples with higher porosity, measured permeabilities of pristine simulant were higher than those of PBX 9501. In this case the difference was one order of magnitude. Even with the initial difference in porosity, the simulant is valuable when its behavior is compared quantitatively to other simulant samples and qualitatively to PBX 9501 samples.

Permeability of simulant that was damaged unconfined compared to pristine simulant shows a three order-of-magnitude increase (compared with a five order increase for PBX 9501). Furthermore, simulant damaged in confinement at 180°C increased in permeability by only two orders of magnitude from its pristine condition (compared with a three order difference for confined PBX 9501 at 180°C). Both of these observations indicate that PBX 9501 damages more severely than the simulant when heated to 180°C. The $\beta - \delta$ phase transition in HMX is likely the reason for the difference in behavior between HMX and the simulant, and the reason for the permeability change observed here. In addition, loss of gaseous products resulting from reaction and evaporation in the flow may complicate the results at certain temperatures. We have, however, measured HMX mass loss as a function of temperature and have verified that the loss is negligible under these experimental conditions.

Room temperature measurements of simulant damaged unconfined compared to itself at 150 or 180°C show very little change in permeability, indicating less compression at elevated temperatures (Figure 5). Since the simulant does not undergo phase transition, this again lends support to the hypothesis that the phase transition is the primary mechanism driving damage and, therefore, permeability.

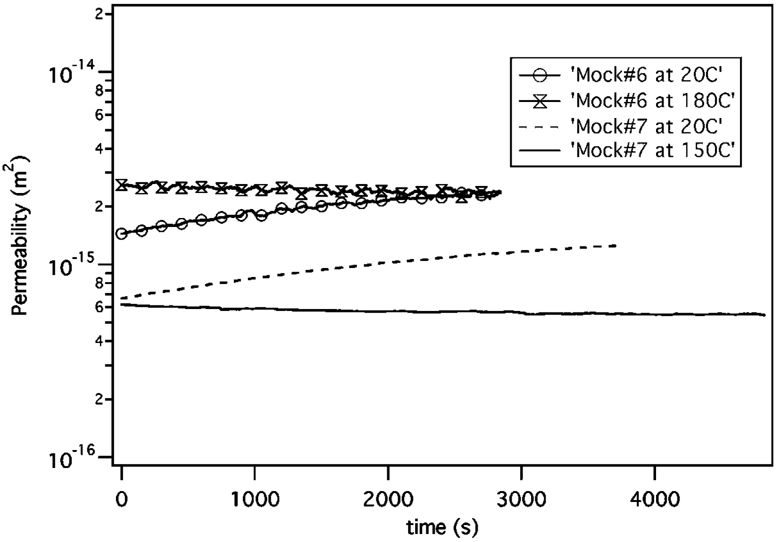

Figure 5. Comparison of permeability measured at 20, 150, and 180°C of two simulant samples that were damaged unconfined. A and B are separate identical samples.

Conclusions

A gas permeameter was developed to make dynamic measurements of energetic materials undergoing thermal damage. When pristine PBX 9501 is heated to temperatures of 180°C, permeability increases by three to five orders of magnitude depending on the level of confinement. Permeability increases for the initial 2–3 hr of heating, after which it attains a quasi-steady permeability. Comparative studies with an ammonium sulfate simulant lend evidence to the conjecture that the HMX $\beta - \delta$ phase transition is likely to be the major mechanism of damage during this initial period. There is evidence for a secondary, long-duration, damage mechanism, the understanding of which is still in progress.

We are currently conducting extensive image analysis using X-ray tomography and photomicrography to define further the morphological changes that result in increased permeability of damaged material.

Acknowledgments

We thank Dave Zerkle and Larry Luck for their contributions to the development of the data reduction scheme and many useful discussions. We acknowledge Drs. Phil Howe and Deanne Idar for the financial support and encouragement of this work.

References

[1] Asay, B. W. et al. 2003. *Journal of Energetic Materials*, 21: 1–13.

[2] Dullien, F. A. L. 1979. *Porous Media: Fluid Transport and Pore Structure*. New York: Academic Press.

[3] Collins, R. E. 1976. *Flow of Fluids through Porous Materials*. Tulsa: Petroleum Publishing Company.

[4] Scheidegger, A. E. 1974. *The Physics of Flow through Porous Media*. Toronto: University of Toronto Press.

[5] ASTM D4525-90, "Standard Test method for Permeability of Rocks by Flowing Air." ASTM Intl. PA.

[6] Shepherd, J. E. and D. R. Begeal. 1988. *Transient Compressible Flow in Porous Materials*. Albuquerque, NM, Sandia National Laboratory.

[7] API. 1956. *Recommended Practice for Determining Permeability of Porous Media*. 3rd ed. New York: American Petroleum Institute.